A Ligand–Ligand Interaction Model for the Structures of Transition Metal Clusters

DARIO BRAGA*
Universita' Degli Studi Di Bologna, Dipartimento Di Chimica 'G. Ciamician', Via Selmi 2, 40 126 Bologna (Italy)
ALISON RODGER
Physical Chemistry Laboratory, South Parks Road, Oxford OX1 3QZ (U.K.)
and BRIAN F. G. JOHNSON
University Chemical Laboratory, Lensfield Road, Cambridge CB2 1EW (U.K.)
(Received January 17, 1990)

Abstract

The model previously applied to the rationalization of simple mononuclear complexes of the type ML_n has been extended to transition metal cluster carbonyls. Application to the series of carbonyls $Mn_2(CO)_{10}$, $Fe_2(CO)_9$, $Co_2(CO)_8$, $Fe_3(CO)_{12}$, $Ru_3(CO)_{12}$, and the two isomers of $Ir_6(CO)_{16}$ reveal the importance of ligand–ligand attractive interactions and that crystal packing forces play an important role in deciding the structure adopted and, in some cases. are sufficient to cause the adopted structure to be different from that expected on the basis of intramolecular forces alone.

Introduction

We have previously developed a model to account for the geometries adopted in ML_n systems [1, 2]. The premises of the model are based on a consideration of the forces that bond a molecule together. The bonding interaction energy between neighbouring atoms is the largest contributor to the stability of a molecule relative to its component atoms. However, this energy does not usually determine the orientation of atoms about a central atom. In this connection the interactions of atoms which are further apart than a bond length, but still comparatively close together, are important. This idea is implicit in any discussion of structure where the phrase 'steric interactions' is used. It is also fundamental to the success of molecular mechanics calculations [3] for both organic and inorganic systems, since such a calculation expresses the energy of a molecule in terms of bond stretches from optimal bond lengths, bends from optimal bond angle values, and atom–atom interactions between non-bonded atoms.

*Author to whom correspondence should be addressed.

Our aim was to understand why a molecule adopts a given ground state geometry. We considered molecules of the form ML_n. We began from the point where all bonds were formed. We assumed that M–L bond strength was essentially independent of the orientation of the L about M (cf. ref. 1 for a discussion of this), and examined the L–L interactions. The L–L interaction was expanded in a multipole-type expansion. At short distance the interaction is dominated by the repulsion due to 'overlapping' electron clouds on atoms. At intermediate distances an attractive dispersion interaction becomes important, and at longer distances (or where the L are charged) an r^{-1} charge–charge interaction (usually repulsive) becomes dominant. The result of this is that the geometry adopted by ML_n for uncharged L is that which enables two Ls not to be forced closer than the sum of their 'hard sphere' (approximation of short range repulsion) radii, but which then maximises their attractive interaction.

It is the purpose of this work to extend this model to transition metal cluster compounds, and to use it to enable us to understand the geometries adopted by particular cluster molecules. If one considers a transition metal complex as a 'zeroth order' cluster then what is required for the extension is apparent. In addition we must remember that the available experimental data is for the solid state, because almost all available structural data is for crystals.

When dealing with solid state structures of neutral transition metal carbonyl clusters most chemists (and most crystallographers) tend to forget that what they are actually looking at is the result of the interplay of three distinct factors: (a) bonding interactions (i.e. chemical bonds in the strict chemical sense) which in a cluster are M–M and M–L bonds; (b) intramolecular non-bonding interactions of the kind mentioned above; and also (c) intermolecular non-bonding interactions which are those holding together the molecules in the crystal. In general (b) are thought of as repulsive and usually discussed in

0020-1693/90/$3.50

terms of minimization of the steric interactions among ligands. However, in light of our work on transition metal complexes an attractive component to that interaction must also be accounted for unless the ligands are so large as to force the M–L bonds to stretch in order to accommodate them. Interactions (c) are usually neglected with or without justification. Again, our experience with transition metal complexes suggests that intermolecular forces can have a small but significant effect on the geometry adopted in the crystal [4] (cf. for example the different twist angles of $[Co(en)_3]^{3+}$ when the counter ions are changed [5]). What is more the effect of intermolecular forces on the molecular shape is well documented by the studies on crystal polymorphism shown by many organic molecules [6].

In order to explore the significance of the three different types of atom–atom interactions in determining what is 'seen' by diffraction experiments we shall express the L–L interactions in terms of atom–atom potentials of the Buckingham type (see below). Such a simple potential will be sufficient to enable us to determine the significance of L–L attractive interactions, and in fact to show that minimizing repulsive interactions is not sufficient to determine the cluster geometries. Crystal packing (that is intermolecular interactions) also prove to play an important role in determining the structure adopted, especially for species showing structural non-rigidity in solution, and in some cases is sufficient to cause the structure adopted not to be that which intramolecular interactions favour [7]. A classic example where higher energy conformations are observed in the solid state again comes from organic solid state chemistry. The angle between the two rings of biphenyl is 42° in the gas phase, while the molecule is planar in the solid state room temperature structure and shows a 10° twist at 22 K [8].

Method

The approach we have adopted to quantify our model is similar to that used by Orpen for hydride location on cluster surfaces [9] and to that used by Hitchcock *et al.* [10] for non-valence interaction computations. All calculations are performed with the program OPEC [11] (Organic Packing Potential Energy Calculations) written by A. Gavezzotti at Milano University.

We express the L–L interaction (both intra and intermolecular) using a potential of the Buckingham type:

$$\sum_i \sum_j [A \exp(-Br_{ij}) - Cr_{ij}^{-6}]$$

where r_{ij} is the interatomic separation between atoms i and j, and A, B, C are parameters which depend on the nature of atoms i and j. The ones used here are [12]

Atom–atom pair	A (kcal/mol)	B (Å)	C (kcal/mol)
O–O	77700	4.18	259.40
C–C	71600	3.68	421.00
O–C	75700	3.91	339.40
Kr–Kr	270600	3.28	3628.00
Kr–O	145002	3.73	970.10

Values for A, B and C are not available for metal bound CO groups, though the literature is full of different parameters for this kind of potential energy calculation. We have adopted values for solid CO in an argon matrix [13], as a similar net charge displacement occurs in these systems and the transition metal complexes and clusters. Dipole–dipole or equivalently charge–charge interactions are not taken into account, since there is almost no net charge on the C and O atoms in carbonyl ligands. (The electron density distributions in $Cr(CO)_6$ is $+0.15 \pm 0.12$ for Cr; $+0.09 \pm 0.05$ for C; and -0.12 ± 0.05 for O [14].) These interactions are envisaged to be more important when we come to include heteroatoms such as halogens.

The intramolecular energy (IAM) is partitioned into the separate C–C, O–O and C–O non-bonding interactions and the repulsive and attractive terms are considered separately. It should be emphasized that this procedure bears no relationship to the atom–atom potential energy method of Pertsin and Kitaigorodsky [15], though use is made of the same Buckingham potential. The main drawback comes from the fitting procedures usually employed to derive values of coefficients by adjusting the potential as a whole to fit some physical property of a crystal (sublimation energy, etc.) or to fit an interatomic potential calculated by *ab initio* methods. The result is that the repulsive and attractive parts of the potential are mixed to some extent after fitting. Thus, our method can only be used on a relative basis to compare closely related species with no pretensions even of obtaining approximate values of non-bonding interactions.

The interactions between nearest neighbour ⟨1–3⟩ atoms (cf. Fig. 1) on the same metal have been omitted from our calculations since they are all close packed and their positions are determined to minimize repulsive forces. Explicitly including them in our calculations tends to obscure the effect of the other interactions. If one were using this approach to determine cluster geometries from first principles rather than to understand the geometry adopted then they must be explicitly included. The non-⟨1–3⟩ metal atom–O contributions are taken

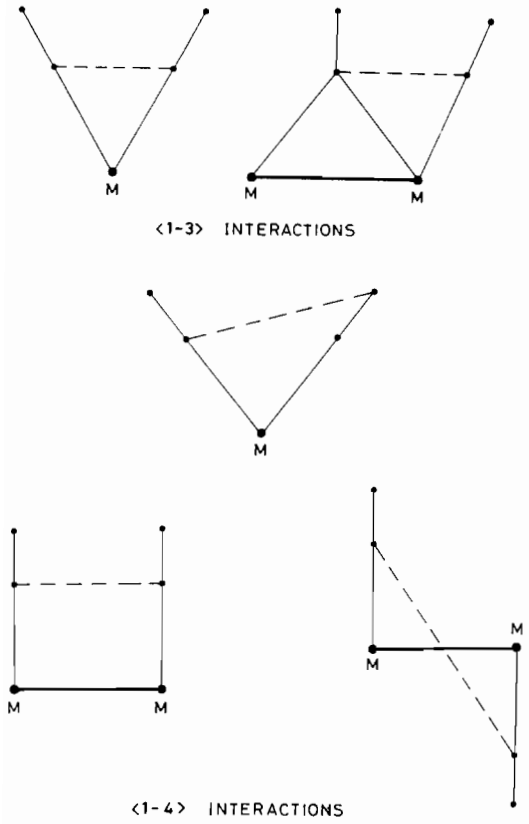

Fig. 1. Schematic representation of some ⟨1–3⟩ and ⟨1–4⟩ interactions.

into account only for first-row metals by using the coefficients of the corresponding noble gas (Kr). The contribution from such interactions is small (cf. Table 1).

In order to test the parameter dependence of the results, the calculations on $Mn_2(CO)_{10}$ (see also below) were carried out with different choices of the coefficient values taken from the literature

O···O	O···C	C···C	Reference
−1.31	−4.76	+3.69	16
−2.37	−5.60	+6.21	17(a)*
−4.65	−10.19	+6.21	17(b)
−0.84	−2.85	−0.51	9**

*From the refinement of succinic anhydride the parameter (a) for =O···O= and –C···C– interactions and the parameter (b) for –O···O– and –C···C– interactions mixed interactions were obtained as $A_{A,B} = (A_A A_B)^{1/2}$; $B_{A,B} = (B_A + B_B)/2$; $C_{A,B} = (C_A C_B)^{1/2}$.
**Note that the potential is in the form $V = A \exp(-Br)/r^6 - C/r^6$.

The results show that although the individual values may vary appreciably, the repulsive/attractive nature of the partitioning does not vary.

The intermolecular energy (IEM) does not need to be partitioned in the same way. We just give a total of all the intermolecular interaction energies between each atom of the reference molecule and the atoms of the surrounding molecules, distributed

TABLE 1. Energetic contributions for the different atom interactions in the clusters studied. C...C interactions are separated into attractive and repulsive contributions

	IAM					IEM		
	O...O	O...C	C...C(rep.)	C...C(attr.)	M...O		Me	p.c.[a]
$Mn_2(CO)_{10}$ (r.t.)	−1.64	−5.08	4.37	−0.66	−1.49	−29.2	−41.1	0.67
$Mn_2(CO)_{10}$ (74 K)	−1.64	−4.87	5.27	−0.68	−1.51	−30.7	−44.7	0.72
$Fe_2(CO)_9$	−1.21	−4.00		−0.28	−0.46	−31.1	−47.5	0.68
$Co_2(CO)_8$ (r.t.)	−0.86	−2.68		−0.36	−0.53	−25.1	−39.4	0.63
mol. 1	−0.87	−2.61		−0.36	−0.53			
mol. 2	−0.86	−2.76		−0.36	−0.53			
$Co_2(CO)_8$ (100 K)	−0.86	−2.76		−0.34	−0.54	−26.0	−41.8	0.66
mol. 1	−0.86	−2.71		−0.33	−0.52			
mol. 2	−0.86	−2.81		−0.34	−0.55			
$Re_2(CO)_{10}$ (r.t.)	−1.41	−4.86	1.82	−0.54		−28.4		
$Fe_3(CO)_{12}$	−2.23	−5.26	7.52	−1.18	−2.75	−34.6		0.66
$Ru_3(CO)_{12}$	−1.58	−4.47	8.23	−1.44	−3.80	−36.6	0.71	
$Ir_6(CO)_{16}$ 'black'	−2.49	−7.47	2.63[b]			−42.3		0.65
μ_2 mol. 1	−2.50	−7.44						
μ_2 mol. 2	−2.48	−7.49						
'red'	−2.69	−8.46	−0.11[b]			−39.1		0.60

[a]Packing coefficients are defined as $V_{molecule}Z/V_{cell}$ (see ref. 6). [b]Not partitioned into repulsive and attractive components.

according to crystal symmetry and falling within 10 Å from the reference one. For all species discussed below, atomic coordinates and space groups are taken from the original structure reports.

Results and Discussion

Before discussing the detailed results from calculations on specific molecules we can make the following general comments from the data results summarized in Table 1. The O–O IAM is always attractive. The O–C IAM is almost always attractive, the exceptions we found being for $Fe_2(CO)_9$ and $Co_2(CO)_8$ where the IAM between bridging and very close nearest-neighbour terminal COs is slightly repulsive (as one might expect). The ⟨1, 4⟩ (cf. Fig. 1) O–C IAM is generally repulsive between COs which are nearest neighbours but not bound to the same metal; C–C IAMs between atoms which are further apart are attractive. The total IAM is usually negative (i.e. attractive) and if positive only slightly so. As an aside it should be noted that if the nearest neighbour C–C interactions had all been included (see above for a discussion of this) then, as Mason found, the total IAM is always repulsive.

Specific Systems

(Note: all numbers are in kcal/mol unless otherwise specified.)

$Mn_2(CO)_{10}$

There are two accurate structural determinations of $Mn_2(CO)_{10}$ besides the early one of Dahl and Rundle [18], one at room temperature (r.t.) [19] and one at 74 K [20]. The staggered conformation and the slight bending of the CO ligands towards the opposite metal atom (see Fig. 2) has been the matter of many disputes on the nature of the bonding between the atoms. From our calculations we see that the total attractive (O–O + O–C + attractive C–C) terms sum up to −7.38 and −7.19 at r.t. and low temperature (l.t.), respectively. Thus, CO ligands on different metal atoms essentially attract each other. Repulsive interactions are confined to C–C interactions and amount to +4.37 and +5.27 at the different temperatures.

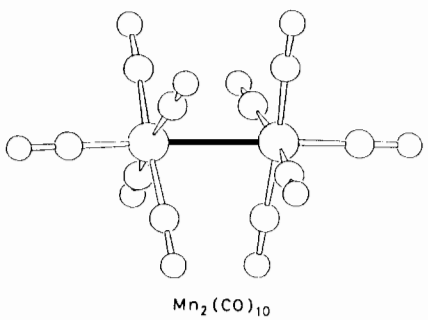

Fig. 2. The molecular structure of $Mn_2(CO)_{10}$.

As one migh expect the crystal packing shrinkage on passing from room temperature to low temperature results in a slight decrease of the Mn–Mn distance (from 2.904 to 2.895 Å) accompanied by a decrease in the attractive part of IAM and an increase in the repulsive part. Again, not unexpectedly, the IEM becomes more stabilizing (decreasing from −29.2 to −30.7) when the temperature is reduced reflecting the fact that the short range repulsion plays little part in determining the IEM. If the metal atom–other atom interactions are 'simulated' by treating Mn as Kr a further attractive term is added to both the IEM and IAM.

We investigated the effect of an eclipsed CO ligand distribution in the IEM in two ways (using the r.t. data). We first determined the effect of rotating one $Mn(CO)_5$ unit 45° about the Mn–Mn bond. The result was a significant increase in the O–C interactions, in addition the O–O interactions become repulsive (+11.54 and +3.89, respectively). We then considered a model structure in which COs bound to the same Mn atom are eclipsed but perpendicular to the Mn–Mn bond. In this model compound, the attractive interactions were smaller than in the real molecule (O–O −1.00, O–C −5.07) as were the C–C repulsions for which we explicitly accounted – so the effects counteract. However, this provides a good example of the necessity of including all C–C interactions if one wishes to determine a geometry from first principles since this model geometry has nearest neighbour C–C contacts for Cs bound to the same metal atom of 2.561 and 2.593 Å (radial–radial and radial–axial respectively), and hence a dominant ⟨1–3⟩ C–C repulsive interaction.

$Re_2(CO)_{10}$

The fact that the $M(CO)_5$ groups are further apart (Re–Re 3.041 Å) [19] than in the previous example results in a decrease in both attractive and repulsive IAM terms and a small decrease in the attractive IEM term with respect to $Mn_2(CO)_{10}$ (−28.4 versus −29.2). As the attractive interactions are longer range than the repulsion terms the net effect on the structure is stabilizing.

$Fe_2(CO)_9$ [21] and $Co_2(CO)_8$ [22]

If the ⟨1–3⟩ interactions involving the bridging ligands of both species (see Fig. 3) are not considered (they are close packed), the IAM results in an overall attraction among the ligands, though O(terminal)–C(bridge) interactions between neighbouring ligands are slightly repulsive in $Co_2(CO)_8$ slightly reducing the net attractive contribution of these interactions. Decreasing the temperature for $Co_2(CO)_8$ [23] does not result in an appreciably

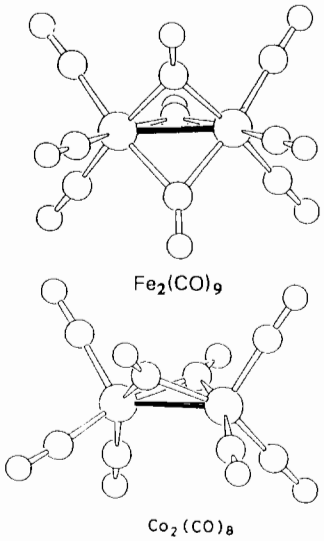

Fig. 3. The molecular structure of $Fe_2(CO)_9$ and $Co_2(CO)_8$.

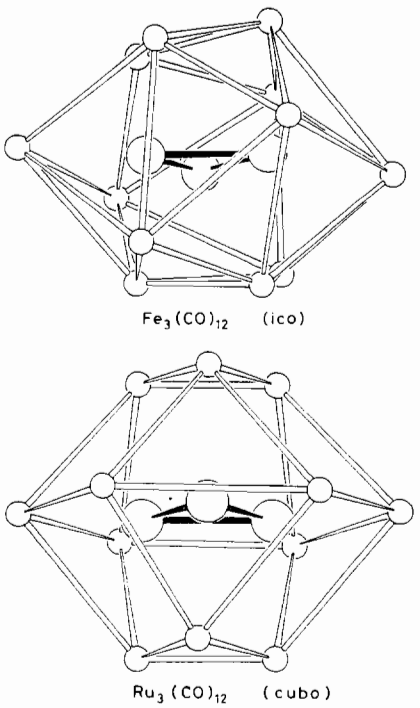

Fig. 4. The quasi-icosahedral ligand envelope of $Fe_3(CO)_{12}$ and the anti-cubo-octahedral one of $Ru_3(CO)_{12}$.

less stable molecular unit and there is a slight gain in the IEM (−25.1 at r.t. versus −26.0 at 100 K). This reflects the 'loose' nature of the crystal packing for this cluster (its packing coefficient is 0.63). In fact its packing is very similar to that of $Fe_2(CO)_9$ (packing coefficient 0.68) but it has a hole instead of the ninth CO [6].

$Fe_3(CO)_{12}$ [24] and $Ru_3(CO)_{12}$ [25]

For these molecules, IAM calculations can be used as a basis for discussing the relationship between the quasi-icosahedral (icos) ligand distribution of the iron cluster and the anti-cubo-octahedral (cubo) one of the ruthenium cluster (see Fig. 4). In both $Fe_3(CO)_{12}$ and $Ru_3(CO)_{12}$ O–O and O–C interactions are attractive (see Table 1). The C–C interactions are more complicated. In $Fe_3(CO)_{12}$ the repulsions are mainly determined by axial–axial and axial–bridge interactions (+7.52), while in $Ru_3(CO)_{12}$ repulsions are due only to axial–axial interactions (+8.23). Since the Fe–Fe bond lengths are much smaller than those of the ruthenium cluster (Fe–Fe 2.639 Å, Ru–Ru 2.854 Å) the reason for the different structures adopted becomes apparent: if $Fe_3(CO)_{12}$ adopted the cubo geometry the axial–axial repulsion would be very strong (in a simple model-structure with only terminal ligands (cubo) the repulsive term increases to 25.5). It is interesting to note that the crystal packing seems to favour the cubo ligand distribution over the icos for the Ru cluster (see Table 1), in agreement with the values of the packing coefficients of the two species (0.66 and 0.71, respectively) [6].

$Ir_6(CO)_{16}$ black (μ-2 bridges) and red (μ-3 bridges)

The isomeric pair of $Ir_6(CO)_{16}$ clusters (see Fig. 5) [26] represents another example of the interplay between the intramolecular and intermolecular interactions in determining the final geometry. (Note that two independent 'half' molecules are present in crystals of the black isomer so that all IAM terms

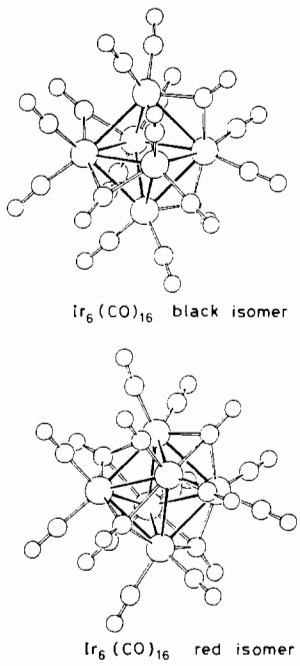

Fig. 5. The 'black' and 'red' isomers of $Ir_6(CO)_{16}$.

described in the following were averaged over corresponding sets of values in the two independent units. Distinct values are reported in Table 1 for comparison.) It can be seen that both O–C and O–O terms favour the red isomer over the black isomer (O–O, – 2.49 versus –2.69; O–C, –7.47 versus –8.46). As the ⟨1 – 3⟩ C–C interactions are different in the two clusters we should include them in our comparisons: if all C–C interactions are included (i.e. including the ⟨1–3⟩ interactions), the red isomer is more stable by about 7 kcal/mol (Although the barrier to inversion is large as the isomers do not readily interconvert), whereas if the ⟨1–3⟩ interactions are ignored the difference is only 2.74. Thus, in total the IAM favours the μ-3-bridged isomer. However, the IEM favours the black isomer by about 3.20 kcal/mol due to the slightly looser packing of the red isomer (packing coefficient of red is 0.60 and of black is 0.69). Thus our previous inference [6] that the two forms are only observed because of cancelling effects from the intramolecular and crystal packing interactions is substantiated.

Conclusions

By examining atom–atom interactions we have been able to gain insight into the factors that are involved in determining the geometry that a number of carbonyl clusters adopt. In general C atoms on a given molecule are close packed and their interaction energy is repulsive. The O–C interactions between non-bonded atoms is almost always attractive, and the O–O interactions are always attractive. The basic assumption of the method outlined here is that the interatomic interactions are 'central' (i.e. they depend only, or mainly, upon the distance between atom centres). This is certainly a crude approximation if one were seeking an accurate representation of the conformational energies of flexible molecules. Although the molecules considered herein are flexible, most of them being extremely fluxional in solution, by using data from crystals, we have confined the analysis to a condition of molecular rigidity. This is not to say that the atoms are fixed in the lattice, but only that they do not have the ease of motion (migration, rotation, tumbling) typical of solution so the forces at work between non-bonded atom pairs can be thought to be similar whether atoms belong to the same or different molecules. In other words we are saying that the factors controlling close-packing of molecules in the crystal do not differ (very much) from those controlling close-packing of ligands around a metal framework. In this respect our approach represents an extension of the hard-sphere approach successfully used earlier to understand (rather more qualitatively) the geometries adopted by simple binary carbonyls [27]. The 'central' interaction used is also too simplistic if the geometry of a molecule forces atoms whose non-bonded electron density are not uniform to be close packed (cf. for example the 'stereoelectronic effects' observed in acetals [28]).

We have also shown that the crystal structure may not be the unique potential energy minimum. For flexible molecules, for which there is a number of possible molecular geometries in solution, the differences in packing arrangements (i.e. in the IEM contribution) can 'pilot' the structural choice in the solid state among different molecular geometries close to the 'global' energy minimum.

More examples of the kind studied in this work can be envisaged and will be a matter of future studies. In particular the effects of heteroatoms on experimental geometries needs to be explored. For many heteroatom–heteroatom interactions it will not be sufficient to consider only the short range repulsions and intermediate range attractions; the longer range charge–charge [1] interactions must also be considered.

References

1 A. Rodger and B. F. G. Johnson, *Inorg. Chim. Acta, 146* (1988) 37.
2 A. Rodger and B. F. G. Johnson, to be published.
3 D. B. Boyd and K. B. Lipkowitz, *J. Chem. Educ., 59* (1982) 269; G. J. McDougall, R. D. Hancock and J. C. A. Boeyens, *J. Chem. Soc., Dalton Trans.*, (1978) 1438.
4 V. G. Albano, D. Braga and F. Grepioni, *Acta Crystallogr., Sect. B, 45* (1989) 60.
5 D. L. Keppert, *Prog. Inorg. Chem., 23* (1979) 1, and refs. therein.
6 J. Bernstein, in G. R. Desiraju (ed.), *Organic Solid State Chemistry*, Elsevier, New York, 1987, pp. 471–510.
7 D. Braga and F. Grepioni, *Acta Crystallogr., Sect. B, 45* (1989) 378.
8 W. R. Busing, *Acta Crystallogr., Sect. A, 39* (1983) 340.
9 A. G. Orpen, *J. Chem. Soc., Dalton Trans.*, (1980) 2509.
10 P. B. Hitchcock, R. Mason and M. Textor, *J. Chem. Soc., Chem. Commun.*, (1976) 1047.
11 A. Gavezzotti, *J. Am. Chem. Soc., 105* (1983) 5220.
12 K. Mirsky, in *Computers in Crystallography, Proc. Int. Summer School Crystallographic Computing*, Delft University Press, Twente, 1978, p. 169; A. Gavezzotti, *Nouv. J. Chim., 6* (1982) 443.
13 K. Mirsky, *Chem. Phys., 40* (1980) 445.
14 B. Rees and A. Mitschler, *J. Am. Chem. Soc., 98* (1976) 7918.
15 A. J. Pertsin and A. I. Kitaigorodsky, *The Atom–Atom Potential Method*, Springer, Berlin, 1986.
16 J. Sanz-Aparicio, S. Martinez-Carrera, Garcia-Blanco and A. Conde, *Acta Crystallogr., Sect. B, 44* (1989) 259.
17 D. Bougeard, R. Righini and S. Califano, *Chem. Phys., 40* (1979) 19.
18 L. F. Dahl and R. E. Rundle, *Acta Crystallogr., 16* (1963) 419.
19 M. R. Churchill, K. N. Amoh and H. J. Wasserwan, *Inorg. Chem., 20* (1981) 1609.

20 M. Martin, B. Rees and A. Mitschler, *Acta Crystallogr., Sect. B, 38* (1982) 6.
21 F. A. Cotton and J. M. Troup, *J. Chem. Soc., Dalton Trans.*, (1974) 800.
22 A. A. Sumner, H. P. Klug and L. E. Alexander, *Acta Crystallogr., 17* (1964) 732.
23 P. C. Leung and P. Coppens, *Acta Crystallogr., Sect. B, 39* (1983) 535.
24 F. A. Cotton and J. M. Troup, *J. Am. Chem. Soc., 96* (1974) 4155.
25 M. R. Churchill, F. J. Hollander and J. P. Hutchinson, *Inorg. Chem., 16* (1977) 2655.
26 S. Garlaschelli Martinengo, P. L. Bellon, F. Demartin, M. Manassero, M. Y. Chiang, C. Y. Wei and R. Bau, *J. Am. Chem. Soc., 106* (1984) 6664.
27 R. E. Benfield and B. F. G. Johnson, *Transition Met. Chem., 6* (1981) 131.
28 P. Deslongchamps, *Stereoelectronic Effects in Organic Chemistry*, Pergamon, Oxford, 1983.